



Partitioning of arterial tree for parallel decomposition of hemodynamic calculations

Andrew Svitenkov¹, Pavel Zun¹, Oleg Rekin¹ and Alfons G. Hoekstra²

¹*ITMO University, St. Petersburg, Russia*

²*Universiteit van Amsterdam, Netherlands*

svitenkov@yandex.ru, pavel.zun@gmail.com, oleg.rekin@gmail.com, a.g.hoekstra@uva.nl

Abstract

Modeling of fluid mechanics for the vascular system is of great value as a source of knowledge about development, progression, and treatment of cardiovascular disease. Full three-dimensional simulation of blood flow in the whole human body is a hard computational problem. We discuss parallel decomposition of blood flow simulation as a graph partitioning problem. The detailed model of full human arterial tree and some simpler geometries are discussed. The effectiveness of coarse-graining as well as pure spectral approaches is studied. Published data can be useful for development of parallel hemodynamic applications as well as for estimation of their effectiveness and scalability.

Keywords: hemodynamics, vascular net, scalability, graph partitioning, coarse-graining, spectral methods, hill-climbing

1 Introduction

Computational modelling is being increasingly used for biomedicine applications (Winslow, Miller, 2012). One important set of applications is modelling the heart and the vascular system (Wootton, 1999; Taylor, 2004). Many highly advanced examples, which are at the same time close to clinical practice, related to the development, progression, and treatment of cardiovascular disease can be found among them (Tarbell, 2003; Vieira, 2015). The key role of fluid mechanics for vascular system models renders computational hemodynamics a vast and growing field (Sforza, 2009; Taylor, 2013). Many biologically significant features of blood flow cannot be reproduced by approximated hemodynamic models (Reymond, 2013) and full 3D blood flow simulations are required. Possible restrictions on the time of solving in some medical applications make modelling of the heart and vascular system an advanced computational problem. Building multiscale models (Lee, 2012) can be a possible way of improving computational efficiency, however, on the other hand, since the particular

task of simulating blood flow can be considered as a problem of PFLOPS scale (Grinberg, 2012), effective use of parallel computational resources becomes a critical part of the problem.

Blood flow modelling is different from many conventional hydrodynamics simulations in the sense that the flow domain is often very complex, that is, highly tortuous with many branches and several inlets and outlets. A space decomposition of hydrodynamics problem on such complex domain can result in a very suboptimal configuration with high communication costs and load imbalances. This happens even for relatively simple flow domains like aneurisms (Chopard et al., 2010), and for a full-body model the result should be even worse. For aneurisms though, covering the flow domain with cubic block structure can result in a rather good partition. However, heterogeneity of whole-body networks makes this approach futile.

In this study we discuss the formulation of the problem of parallel decomposition of blood flow simulation domain as graph partitioning problem. We reduce the 3D mesh of vascular system to 1D network, which is then interpreted as a graph, partitioned in a way that minimizes communication and assigned to the processors to compute blood dynamics.

2 Related work

The problem of graph partitioning is a well known. Theoretically it is itself an NP-complete problem (Garey et al, 1976). However, a lot of heuristic algorithms which show reasonably good results on many graphs from different real-life domains were suggested and applied (Safro et al, 2012; LaSalle et al, 2015; Karypis et al, 1988). Some major types of partitioning methods can be distinguished (Buluç, 2013).

The main approaches are coarse-graining the graph to solve the partitioning problem for a smaller number of nodes and then refine it (Safro et al, 2012; Karypis et al, 1988); geometrical methods, which split the graph according to spatial coordinates of the nodes (if such coordinates exist) (Gilbert et al, 2007); spectral methods, which are often used as an intermediate step of coarse-grained schemes; and genetic algorithms (Steenbeek et al, 1998). Some attempts are made to utilize max-flow min-cut theorem to find minimal cut via flow. This approach ignores balance completely, but it can produce good results for regular random graphs (Bui et al, 1987). Also, for some classes, for example planar graphs, exact solutions can be found in polynomial time (Seidel, 2005).

All methods are well represented in studies and the features of applying them to various types of graph are known in general. Despite that, we believe that the issue of partitioning the arterial network has to be considered separately. First of all, the graph based on 1D arterial network has some noticeable features, which cannot be recognized using the common characteristics of graphs such as average degree of vertex, centrality, diameter and etc. While the effectiveness of partition algorithms for various types of graphs is usually classified by these characteristics (LaSalle et al, 2015), extrapolation of these results to the arterial graph is hardly possible. Additionally the common major objectives of developing partitioning algorithms are different from ours. Whereas the performance and parallelization of algorithms is often critical (Benlic, 2011; LaSalle, Karypis, 2015), our graphs are small enough (thousands of vertices) to neglect this issue. Quality of partitioning and its imbalance, on the other hand, are absolutely critical for the obtainable parallel effectiveness of the hypothetical calculation performance.

We apply graph partitioning techniques to anatomical arterial structures to obtain balanced partitions with minimal interconnections. In biomedical disciplines, the graph partitioning problem usually comes up in the context of image recognition and area detection (see for example (Song et al., 2015; Almasi et al., 2014)). When vascular trees have to be partitioned for various purposes, it is usually done by hand or semi-automatically, based on anatomical classification (Malossi et al, 2012; Passerini et al, 2009; Reymond et al, 2009). We aren't aware of any systematic studies of automatic partitioning of large vascular trees.

However, the wide and well studied range of graph partitioning methods allows us to choose some of the most effective among them with the account to the main features of the vascular network. Thus we assume three main features of the considered network: global symmetry (left-right), strong heterogeneity of scales (compare vascular networks in the thigh and in the brain), and weak connectivity. Heterogeneity and hierarchy of scales suggest that using the coarse-graining (CG) approach is a sensible choice. We consider a typical but recent coarsening scheme suggested by Safro et al. (Safro et al, 2014). Spectral partitioning methods look more suitable for our problem (Mohar, 1991; Spielman, Teng, 2007) than geometric ones (Gilbert et al, 2007) since general symmetry and hierarchy can be taken into account in spectral approach. The refinement hill-scanning method (LaSalle, 2015) was chosen because it is a recent and deterministic algorithm which makes analysis easier. Additionally, a clearly adjustable level of greediness is desirable for applying it to weakly connected graphs.

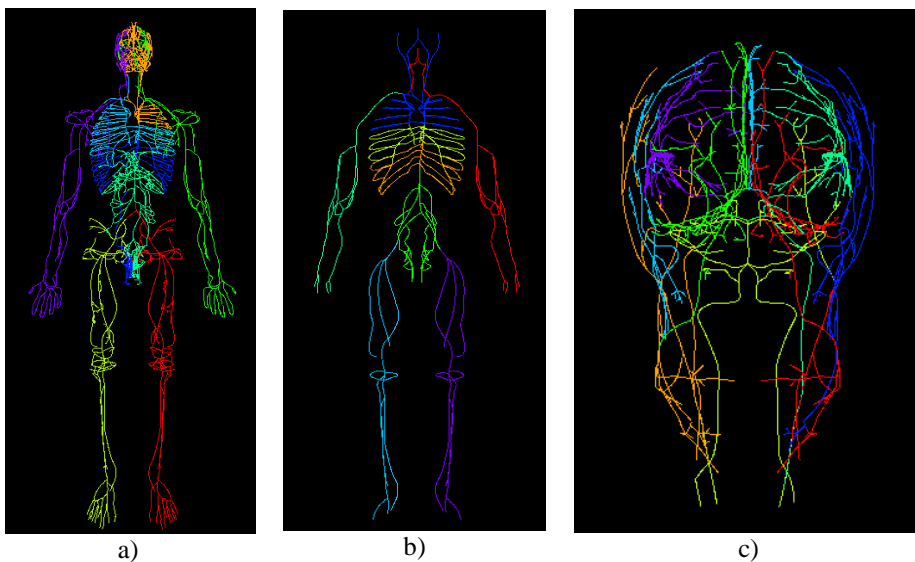


Figure 1: Considered arterial models: (a) high-resolution whole body network; (b) low-resolution whole body network; (c) high-resolution head and neck vessels. The best found partitioning on 8 parts is illustrated by color

3 Methodology

3.1 One-dimension representation of vascular networks

The vessel geometry was obtained from anatomical three-dimension networks. The base model was taken from (Karsakov, 2014). In these networks, first the centerline was detected, and then the vertices were placed on this geometry to split it into fragments suitable for computing the flow. The size of the fragments was aligned. It can be noted that results of decomposition of such linear geometry can be used for 1D approaches as well as for 3D calculations. Volumetric domains are obtained by inverse transform procedure for centerline model.

We have used three different vascular domains for our computations: a high-resolution whole body network (HRWB) of 21312 vertices, a low-resolution whole body network (LRWB), 2129 vertices, and a high-resolution head and neck vessels (HRH), 3278 vertices. The models are shown in Figure 1. For HRWB the distance between vertices of the graph equals 2.5 mm, for LRWB the same distance is

10 mm. The high-resolution whole body network is a highly heterogeneous domain with hierarchical structure which includes complex clusters of small arteries (like for the head) connected by small number of large arteries (such as the aorta). It reduces the amount of effective cuts (with small edgcut) and presents the challenge to a partitioning algorithm. For comparison, we separately use the head vessels, which have a much smaller scale difference between them. Also, the simplified whole body model has been tested. First, this model brings us closer to the current whole-body flow simulations (Mynard, 2008) which do not model small vessels explicitly. Second, the scale of the vessels is even more uniform for this geometry than for the high-resolution head model, and third, the low-resolution geometry serves well to demonstrate and analyze regions that cause most problems for partitioning algorithms.

3.2 Algorithms

Since multi-step heuristic algorithms seem to be the most effective, we explore three typical levels of such algorithms. For coarse-graining we use a single recent method, which is based on utilizing the Galerkin operator (Safro et al., 2014). Two main ideas that cause this coarsening algorithm to yield good results are: the AMG approach, which works well with complex graphs, which are placed in the second and the third sets; a specific way to calculate connectivity strength between nodes, that leads to better quality of partitioning at the cost of increased running time (Safro et al., 2014; Ron et al, 2011).

The CG algorithm we use has following parameters. Parameters of algebraic distance calculation factor in relaxation matrix formula $\alpha=0.5$, count of test vectors $R=5$, count of relaxation iterations $k=20$. Another parameter relates to the AMG part of the algorithm and denotes coupling strength $\theta=0.5$. The imbalance factor is $\epsilon=0.03$ (Safro et al., 2014).

For the second stage, two different spectral methods were used.

The basic spectral algorithm consists of computing the discrete graph Laplacian L , 2^{nd} -smallest eigenvalue of L and its associated eigenvector \mathbf{f} (Fiedler vector). The graph is split so that the vertices associated with small values in \mathbf{f} are in one part, and those associated with large values are in another one (Mohar, 1991; Spielman, Teng, 2007). The median value in \mathbf{f} was chosen as the splitter, so that the resulting parts were balanced.

This algorithm can only split the network in two parts. It can be extended to obtain a larger amount of parts in two different ways.

Cascade partitioning is *the first one*. Its idea is to apply spectral bisection recursively to each part produced by the previous iteration, until the required amount of parts is obtained.

The second one is a generalization of spectral octasection (Hendrickson, Leland, 1995). Instead of using the Fiedler vector, this algorithm uses the k eigenvectors corresponding to k smallest eigenvalues (starting from the 2^{nd} -smallest) to assign the vertices to 2^k parts. The drawback of this method is that we cannot use the eigenvector coordinates directly. Instead, to optimally assign the vertices to 2^k parts, we have to solve a minimal cost assignment problem in k -dimensional space (Tokuyama, Nakano, 1991). The strength of this algorithm is that it assigns all vertices in one iteration.

The last step is the refinement of the coarse splitting. One of the most recent algorithms is given by (LaSalle et al, 2015) and was chosen for being deterministic and its ability to regulate its greediness. This approach allows for breaking out of local minima by moving vertices that increase the edgcut (weight of the edges that connect different parts of the graph) on their own, but decrease it when these vertices are moved as a whole. This capability is known as *hill-climbing*. The capabilities of the chosen algorithm are depicted in Figure 2. Case (a) is a result of partitioning of low-resolution whole body network by cascade spectral algorithm before refinement. Fourth part is located mostly in legs (isn't shown) and is colored green. The "bad" part of it is clearly visible on the right side of the chest, but is fully corrected by the refinement procedure.

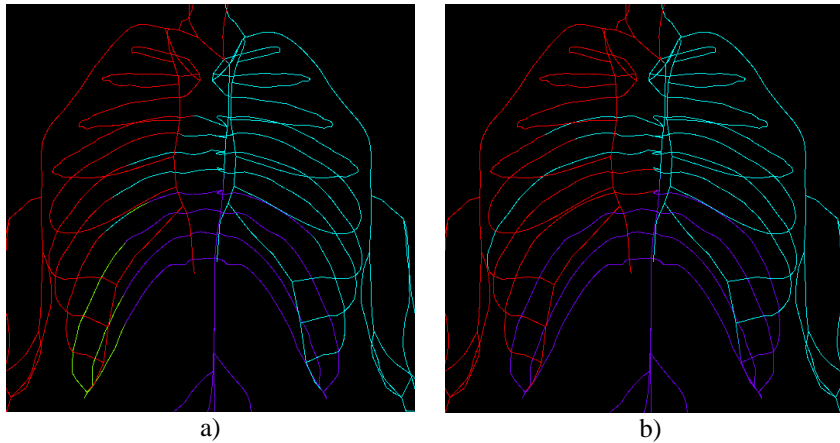


Figure 2: Partitioning of low-resolution whole body network: (a) before refinement procedure; (b) after refinement procedure (4th part placed below and isn't shown)

4 Calculations

Some combinations of the listed algorithms were used for computational experiments. The special notation used for their designation is described here. The coarse-grain procedure is denoted by CG- X , where X is the maximum number of CG blocks (the real number is usually a little lower). The algorithm based on spectral octasection is denoted by SO- Y , where Y is the number of parts. Due to the restriction of the partition procedures Y equals to 2^k , where k is a natural number. Cascade spectral partition procedure is denoted by CAS- Y , and RF denotes the refinement procedure. Thus, for example, the combination CG-512 CAS-32 RF means that the original vascular network was coarse-grained with the upper bound of 512coarse-grained vertices, divided into 32 parts and then the refinement procedure was applied.

4.1 Low-resolution whole body network

The results of applying CAS- Y partition algorithm to the low-resolution whole body network are presented in Table 1. The "+" sign in the RF column denotes the application of the refinement procedure.

Number of partitions, Y	Average size of a partition, N	Standard deviation of N	Average edgecut C	Standard deviation of C	RF
4	532.5	0.1%	9.00	16.2%	-
		0.1%	6.75	32.8%	+
8	266.3	4.8%	6.88	27.4%	-
		6.8%	4.63	48.9%	+
16	133.1	1.1%	8.06	40.3%	-
		8.4%	4.31	40.3%	+
32	66.6	8.4%	5.19	58.5%	-
		13.0%	3.50	44.1%	+
64	33.3	8.5%	3.84	31.8%	-
		13.3%	2.83	54.7%	+

Table 1: Application of CAS- Y partition to the low-resolution whole body (LRWB) model

The results of applying the CG-512 SO- Y partition algorithm to the low-resolution whole body network are collected in Table 2.

Number of partitions, Y	Average size of a partition, N	Standard deviation of N	Average edgecut C	Standard deviation of C	RF
4	532.5	4.4%	9.00	32.7%	-
		4.1%	5.00	36.5%	+
8	266.3	6.2%	7.88	46.7%	-
		6.2%	3.63	46.7%	+
16	133.1	8.9%	7.13	42.5%	-
		12.2%	4.25	54.0%	+
32	66.6	14.8%	6.72	47.1%	-
		10.0%	3.66	37.2%	+
64	33.3	16.1%	5.77	48.1%	-
		9.1%	3.09	50.4%	+

Table 2: Application of CG-512 SO- Y partition to the LRWB model

4.2 High-resolution whole body network

The results of applying the CAS- Y partition algorithm to the high-resolution whole body (HRWB) network are collected in Table 3. Table 4 collects the results of applying the CG-4096 CAS- Y , and Table 5 shows the CG-X-SO- Y algorithm. The number of blocks X is shown in an additional column in Table 5.

Number of partitions, Y	Average size of a partition, N	Standard deviation of N	Average edgecut C	Standard deviation of C	RF
128	166.5	8.1%	7.01	45.1%	-
		10.1%	3.90	48.1%	+
256	83.2	12.2%	6.35	42.0%	-
		12.0%	3.15	46.8%	+
512	41.6	12.5%	5.06	48.1%	-
		12.0%	2.25	49.5%	+

Table 3: Application of CAS- Y partition to the HRWB model

Number of partitions, Y	Average size of a partition, N	Standard deviation of N	Average edgecut C	Standard deviation of C	RF
256	83.2	13.6%	6.63	43.0%	-
		11.2%	3.16	45.7%	+
512	41.6	18.7%	5.28	45.1%	-
		14.9%	2.46	47.6%	+

Table 4: Application of CG-4096 CAS- Y partition to the HRWB model

4.3 High-resolution head arterial network

Tables 6, 7 and 8 collect the results of applying partition procedures to high-resolution head arterial network.

Num. of partitions, Y	Av. size of a partition, N	Min. num. of CG blocks	Standard deviation of N	Average edgecut C	Standard deviation of C	RF
4	5326.8	512	7.1%	10.50	41.0%	-
			6.0%	5.75	47.2%	+
8	2663.4	512	8.2%	9.06	60.9%	-
			8.1%	4.75	51.3%	+
16	1331.7	512	11.8%	7.59	48.6%	-
			10.0%	4.59	44.7%	+
32	665.8	512	19.2%	6.66	56.3%	-
			9.5%	4.58	52.0%	+
64	332.9	2048	10.3%	6.60	45.1%	-
			10.3%	3.90	42.4%	+
128	166.5	2048	18.6%	5.81	45.1%	-
			9.2%	3.50	44.7%	+
256	83.2	2048	7.1%	10.50	41.0%	-
			6.0%	5.75	47.2%	+

Table 5: Application of CG-X SO-Y partition to HRFB model. The partition corresponding to the gray-filled values is shown on the Figure 1a.

Number of partitions, Y	Average size of partition, N	Standard deviation of N	Average edgecut C	Standard deviation of C	RF
8	409.9	3.9%	6.50	28.5%	-
		7.2%	4.13	39.8%	+
32	102.5	2.3%	5.19	47.3%	-
		5.9%	3.38	57.2%	+
64	51.2	15.3%	3.86	41.8%	-
		17.2%	2.64	56.2%	+
128	25.6	6.2%	3.73	32.8%	-
		10.6%	2.45	46.4%	+

Table 6: Application of CAS-Y partition to HRH model. The partition corresponding to the gray-filled values is shown on the Figure 1b.

Number of partitions, Y	Average size of partition, N	Standard deviation of N	Average edgecut C	Standard deviation of C	RF
32	102.5	7.7%	6.06	49.7%	-
		4.6%	4.41	49.5%	+
64	51.2	13.7%	4.63	47.9%	-
		9.1%	3.45	47.0%	+

Table 7: Application of CG-512 CAS-Y partition to HRH model

Number of partitions, Y	Average size of partition, N	Standard deviation of N	Average edgecut C	Standard deviation of C	RF
8	409.9	11.7%	6.13	42.2%	-
		14.0%	3.75	48.9%	+
32	102.5	11.4%	6.66	46.8%	-
		4.2%	4.31	48.7%	+
64	51.2	19.4%	4.47	47.7%	-
		16.4%	2.69	47.8%	+

Table 8: Application of CG-512 SO-Y partition to HRH model. The partition corresponding to the gray-filled values is shown on the Figure 1c.

5 Discussion

First of all we can determine the general behaviour of the partitioning procedures in dependence on the number of partitions and the average partition size. Figures 3 a) and b) show the standard deviation of the average partition size and the average edgcut as functions of the number of partitions. We can note the decreasing trend in the edgcut and assume that it approaches the average degree of a vertex as the number of partitions increases and approaches the number of vertices (see additionally Tables 6 and 8). In our case, many vertices lie on linear sites (without bifurcations) of the arterial network, so the average degree of a vertex is close to 2. The dynamic of the standard deviation of the average partition size has an even more interesting appearance. There is a maximum average size of a partition (~ 300 vertices for HRWB, 50 vertices for HRH, 40 vertices or less for LRWB) after which the unbalance of partitions decreases.

Based on the obtained data an analysis of each implemented algorithm can be conducted. For the pure partitioning without final refinement we can notice some benefit of the cascade partitioning algorithm in spite of our expectations. For example, compare CG-512 SO-64 and CG-512 CAS-64 on the HRH model, or CAS-64 and CG-512 SO-64. The benefit of cascade approach is not so definite for the case of the HRWB model, where heterogeneity of scales is stronger. SO algorithm produces better balance especially for small partitions (CG-2048 SO-256, CG-2048 SO-128), while cascade approach, on the other hand, minimizes the edgcut value.

The results of applying the refinement procedure are of special interest. It turns out that the refinement stage is critically important for the quality of the final partitioning and all noticed features of CAS and SO procedures become rather negligible after the refinement step. In most cases, the RF procedure trades the balance of the partition for a decrease in edgcut, especially if the initial partitioning was good. However, we have found that thorough adjustment of RF parameters frequently allows for an improvement in both of these characteristics (CG-512 CAS-64, CG-2048 SO-512 for example). The depth of the search is the most important parameter for this (LaSalle et al., 2015).

The contribution of CG procedure to the final quality of the partition is not very clear. The situation is complicated because a direct application of SO procedure without initial coarse-graining is too computationally hard. For the case of cascade approach, comparing the Tables 3 and 4 on one hand and Tables 6 and 7 on the other gives opposite outcomes. Anyway, there is no doubt about the computational efficiency of the initial coarse-graining procedure.

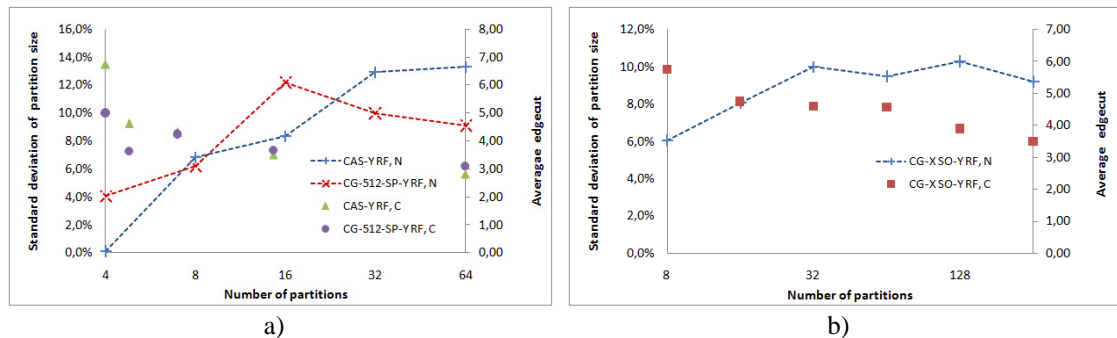


Figure 3: The standard deviation of the average partition size and the average edgcut as functions of the number of partitions for LRWB and HRWB models

6 Conclusions

In this paper we have presented the results of testing different partitioning schemes for real-life vascular networks. We utilize three types of algorithms in the CG multistep partition approach: coarse-graining, partition, and refinement. Two spectral methods were implemented for partitioning. We have shown that graph partitioning approach is applicable for these networks. Remarkable, that spectral methods take in account the anatomical structure of vascular net, that is especially noticeable for partitioning into a small amount of parts.

The cascade spectral method has turned out to produce slightly better results than the direct method, but the refinement levels most of the differences. A combination of the cascade method with refinement produces a slightly smaller cut, and the direct method results in slightly more balanced partitions after refinement. It turns out that the refinement stage is critically important for the quality of the partitioning. The effectiveness of the chosen refinement method (so called *hill-climbing* approach) additionally was shown. Using the initial coarsening does not worsen the result, and in some cases can even improve it.

The amount of inter-part edges per part decreases and approaches the average degree of a vertex with the increase in the amount of parts. The dependency of the balance on the number of partitions is interesting but intuitively clear too. The standard deviation has a maximum for some average value of the partition size and decreases with further decrease of partition size. Generally a standard deviation of 10% is typical for the number of vertices per part. Attempts to decrease this deviation lead to a fast increase in connectivity.

Because of all this, one can presume a sublinear growth of communication expenses with the increase in the number of processing cores, which makes the task of parallelizing whole-body flow simulations a promising one.

Acknowledgments

This paper is financially supported by The Russian Scientific Foundation, Agreement #14-11-00826 (10.07.2014).

This work was partly performed by the Master students (Oleg Rekin) of the Master's Programme in Computational Science (Krzyszczanovskaya et al, 2015).

References

- Almasi, S., Xu, X., Ben-Zvi, A., Lacoste, B., Gu, C., & Miller, E. L. (2015). A novel method for identifying a graph-based representation of 3-D microvascular networks from fluorescence microscopy image stacks. *Medical image analysis*, 20(1), 208-223.
- Benlic, U., & Hao, J. K. (2011). An effective multilevel tabu search approach for balanced graph partitioning. *Computers & Operations Research*, 38(7), 1066-1075.
- Bui, T. N., Chaudhuri, S., Leighton, F. T., & Sipser, M. (1987). Graph bisection algorithms with good average case behavior. *Combinatorica*, 7(2), 171-191.
- Buluç, A., Meyerhenke, H., Safro, I., Sanders, P., & Schulz, C. (2013). Recent advances in graph partitioning. Preprint.
- Chopard, B., Lagrava, D., Malaspinas, O., Ouared, R., Latt, J., Lovblad, K. O., & Pereira-Mendes, V. (2010). A lattice Boltzmann modeling of bloodflow in cerebral aneurysms. In V: European Conference on Computational Fluid Dynamics, ECCOMAS CFD (Vol. 453, p. 12).

- Garey, M. R., Johnson, D. S., & Stockmeyer, L. (1976). Some simplified NP-complete graph problems. *Theoretical computer science*, 1(3), 237-267.
- Gilbert, J. R., Miller, G. L., & Teng, S. H. (1998). Geometric mesh partitioning: Implementation and experiments. *SIAM Journal on Scientific Computing*, 19(6), 2091-2110.
- Grinberg, L., Insley, J. A., Fedosov, D. A., Morozov, V. A., Papka, M. E., & Karniadakis, G. E. (2012). Tightly Coupled Atomistic-Continuum Simulations of Brain Blood Flow on Petaflop Supercomputers. *Computing in Science and Engineering*, 14(6), 58-67.
- Hendrickson, B., & Leland, R. (1995). An improved spectral graph partitioning algorithm for mapping parallel computations. *SIAM Journal on Scientific Computing*, 16(2), 452-469.
- Karsakov, A., Bilyatdinova, A., & Hoekstra, A. G. (2014). 3D virtual environment for project-based learning. In *Application of Information and Communication Technologies (AICT)*, 2014 IEEE 8th International Conference on (pp. 1-5). IEEE.
- Karypis, G., & Kumar, V. (1998). A fast and high quality multilevel scheme for partitioning irregular graphs. *SIAM Journal on scientific Computing*, 20(1), 359-392.
- Krzyszhanovskaya, V.V., Dukhanov, A.V., Bilyatdinova A., Boukhanovsky A.V., & Sloot P.M.A. (2015). Russian-Dutch double-degree Master's programme in computational science in the age of global education, *Journal of Computational Science*, 10, 288-298.
- LaSalle, D., & Karypis, G. (2015). A Parallel Hill-Climbing Refinement Algorithm for Graph Partitioning.
- LaSalle, D., Patwary, M. M. A., Satish, N., Sundaram, N., Dubey, P., & Karypis, G. (2015, November). Improving graph partitioning for modern graphs and architectures. In *Proceedings of the 5th Workshop on Irregular Applications: Architectures and Algorithms* (p. 14). ACM.
- Lee, J., & Smith, N. P. (2012). The multi-scale modelling of coronary blood flow. *Annals of biomedical engineering*, 40(11), 2399-2413.
- Malossi, A. C. I., Blanco, P. J., & Deparis, S. (2012). A two-level time step technique for the partitioned solution of one-dimensional arterial networks. *Computer Methods in Applied Mechanics and Engineering*, 237, 212-226.
- Mohar, B., Alavi, Y., Chartrand, G., & Oellermann, O. R. (1991). The Laplacian spectrum of graphs. *Graph theory, combinatorics, and applications*, 2(871-898), 12.
- Mynard, J. P., & Nithiarasu, P. (2008). A 1D arterial blood flow model incorporating ventricular pressure, aortic valve and regional coronary flow using the locally conservative Galerkin (LCG) method. *Communications in Numerical Methods in Engineering*, 24(5), 367-417.
- Passerini, T., de Luca, M., Formaggia, L., Quarteroni, A., & Veneziani, A. (2009). A 3D/1D geometrical multiscale model of cerebral vasculature. *Journal of Engineering Mathematics*, 64(4), 319-330.
- Reymond, P., Crosetto, P., Deparis, S., Quarteroni, A., & Stergiopoulos, N. (2013). Physiological simulation of blood flow in the aorta: comparison of hemodynamic indices as predicted by 3-D FSI, 3-D rigid wall and 1-D models. *Medical engineering & physics*, 35(6), 784-791.
- Ron, D., Safro, I., & Brandt, A. (2011). Relaxation-based coarsening and multiscale graph organization. *Multiscale Modeling & Simulation*, 9(1), 407-423.
- Safro, I., Sanders, P., & Schulz, C. (2015). Advanced coarsening schemes for graph partitioning. *Journal of Experimental Algorithmics (JEA)*, 19, 2-2.
- Seidel, E., Jansen, K., Karpinski, M., Lingas, A (2005). Polynomial time approximation schemes for max-bisection on planar and geometric graphs. *SIAM Journal on Computing*, 35(1), 110-119.
- Sforza, D.M., C.M. Putman, and J.R. Cebal, Hemodynamics of Cerebral Aneurysms. *Annual Review of Fluid Mechanics*, 2009. 41(1): p. 91-107.
- Song, Y., Zhang, L., Chen, S., Ni, D., Lei, B., & Wang, T. (2015). Accurate Segmentation of Cervical Cytoplasm and Nuclei Based on Multiscale Convolutional Network and Graph Partitioning. *Biomedical Engineering, IEEE Transactions on*, 62(10), 2421-2433.

Spielman, D. A., & Teng, S. H. (2007). Spectral partitioning works: Planar graphs and finite element meshes. *Linear Algebra and its Applications*, 421(2), 284-305.

Steenbeek, A. G., Marchiori, E., & Eiben, A. E. (1998, May). Finding balanced graph bi-partitions using a hybrid genetic algorithm. In *Evolutionary Computation Proceedings, 1998. IEEE World Congress on Computational Intelligence., The 1998 IEEE International Conference on* (pp. 90-95). IEEE.

Tarbell, J.M., Mass Transport in Arteries and the localization of Atherosclerosis, in *Annu. Rev. Biomed. Eng.* 2003. p. 79 - 118.

Taylor, C. A., Fonte, T. A., & Min, J. K. (2013). Computational fluid dynamics applied to cardiac computed tomography for noninvasive quantification of fractional flow reserve: scientific basis. *Journal of the American College of Cardiology*, 61(22), 2233-2241.

Taylor, C. A. and M. T. Draney, *Experimental and Computational Methods in Cardiovascular Fluid Mechanics*, in *Annu. Rev. Fluid Mech.* 2004. p. 197 - 231.

Vieira, M. S., Hussain, T., & Figueroa, C. A. (2015). Patient-Specific Image-Based Computational Modeling in Congenital Heart Disease: A Clinician Perspective. *Journal of Cardiology and Therapy*, 2(6), 436-448.

Winslow, R. L., Trayanova, N., Geman, D., & Miller, M. I. (2012). Computational medicine: translating models to clinical care. *Science translational medicine*, 4(158), 158rv11-158rv11.

Wootton, D. M. and D. N. Ku, *Fluid Mechanics of Vascular Systems, Diseases, and Thrombosis*, in *Annu. Rev. Biomed. Eng.* 1999. p. 299 - 329.